PSYCHOMETRIKA—VOL. 75, NO. 2, 373–390
JUNE 2010
DOI: 10.1007/S11336-010-9159-3

OPTIMIZATION OF BLOCKED DESIGNS IN FMRI STUDIES

BÄRBEL MAUS, GERARD J.P. VAN BREUKELEN, RAINER GOEBEL, AND MARTIJN P.F. BERGER

MAASTRICHT UNIVERSITY

Blocked designs in functional magnetic resonance imaging (fMRI) are useful to localize functional brain areas. A blocked design consists of different blocks of trials of the same stimulus type and is characterized by three factors: the length of blocks, i.e., number of trials per blocks, the ordering of task and rest blocks, and the time between trials within one block. Optimal design theory was applied to find the optimal combination of these three design factors. Furthermore, different error structures were used within a general linear model for the analysis of fMRI data, and the maximin criterion was applied to find designs which are robust against misspecification of model parameters.

Key words: blocked design, fMRI, optimal design, efficiency, maximin.

1. Introduction

Functional magnetic resonance imaging (fMRI) is widely used in cognitive neuroscience to localize human brain functions (Owen, Epstein & Johnsrude, 2003; Chein & Schneider, 2003). It is also applied to determine the related brain areas to psychiatric disorders, e.g., schizophrenia (Honey & Bullmore, 2002). Since its invention in the early 1990s, fMRI has led to major advances in understanding the neural mechanisms that underlie cognitive processes, e.g., perception, attention, language, and memory (Chein & Schneider, 2003). It has established a strong link between cognitive psychology and neuroscientific research. Compared with other neuroimaging methods as, e.g., Positron Emission Tomography (PET), fMRI has advantages in terms of increased spatial resolution (Di Salle, Formisano, Linden, Goebel, Bonavita, Pepino, Smaltino & Tedeschi, 1999). However, one major drawback of fMRI is the low signal-to-noise ratio (SNR). To overcome this weakness, optimal design of fMRI experiments is helpful to increase the signal-to-noise ratio (Josephs & Henson, 1999).

The fMRI signal in most studies is based on the bold-oxygen-level-dependent (BOLD) contrast which is based on magnetic properties of oxygenated and deoxygenated blood and hemodynamic processes like regional cerebral blood flow (rCBF) caused by neural activity (Logothetis & Wandell, 2004). The hemodynamic response to one short stimulus can be described by a hemodynamic response function (HRF) (Friston, Jezzard & Turner, 1994). The double gamma function is mostly employed as HRF and models the temporal evolution of the hemodynamic response over a period of around 30 s (Friston, Fletcher, Josephs, Holmes, Rugg & Turner, 1998). There are mainly two different types of design in fMRI experiments: blocked designs and event-related designs (Aguirre & D'Esposito, 1999; Chein & Schneider, 2003). In blocked designs, trials of one condition are performed in blocks which can be a task condition or a rest condition, i.e., null block, with no systematic or task-related activation. In contrast, event-related designs can have a random order of trials and a fixed or random time interval between trials (Buckner, Bandettini, O'Craven, Savoy, Petersen, Raichle & Rosen, 1996; Dale & Buckner, 1997; Rosen, Buckner & Dale, 1998).

Requests for reprints should be sent to Bärbel Maus, Faculty of Health, Medicine and Life Sciences, Department of Methodology and Statistics, Maastricht University, Maastricht, Netherlands. E-mail: baerbel.maus@stat.unimaas.nl

Blocked and event-related designs are optimal for different purposes, e.g., blocked designs are better for detection of activated brain areas assuming a certain HRF shape, whereas event-related designs are useful to estimate the shape of the HRF (Friston, Zarahn, Josephs, Henson & Dale, 1999; Chein & Schneider, 2003; Birn, Cox & Bandettini, 2002; Liu, Frank, Wong & Buxton, 2001; Liu & Frank, 2004; Liu, 2004). In the fMRI literature, detection of activation is referred to as detection power, whereas estimation of the HRF is called estimation efficiency. In this paper, the focus is on blocked designs and detection power, but this approach can be applied to event-related designs or estimation efficiency as well. Several authors have generated random event-related designs and determined their estimation efficiency (Buračas & Boynton, 2002; Hagberg, Zito, Patria & Sanes, 2001; Wager & Nichols, 2003; Kao, Mandal, Lazar & Stufken, 2009). Maus, van Breukelen, Goebel, and Berger (2010) apply the maximin approach to locally optimal event-related designs for estimation efficiency.

The performance of fMRI experiments is very expensive and time consuming. A scanner session for one subject might take one hour which may cost between $200 and $1000 per hour, not including additional expenses such as subject fees, equipment, and staff salaries (Culham, 2006). The number of subjects and repeated measurements may be restricted due to budgetary constraints. Thus, it is necessary to minimize costs and to maximize the efficiency of the estimators. The purpose of this study is to maximize the efficiency within a fixed budget.

Some general recommendations for blocked designs are given in the fMRI literature. The most simple design is the alternating boxcar design in Figure 1a which consists of alternations between blocks of two conditions. One of these conditions can be a null block where no systematic or task-related stimulation takes place. Thus, the design has the following structure: ANANAN (boxcar design), where A refers to a task condition, and N to a null block, or ABABAB, where A and B refer to two different task conditions. Mohamed, Tracy, Faro, Emperado, Koenigsberg, Pinus, and Tsai (2000) showed that an alternating block order ANANAN was more effective than a continuous design AAANNN. Similarly, Nakai, Matsumura, Nose, Kato, Glover, and Matsuo (2003) showed that although they used the same number of task blocks A and B in each blocked design, detection of functional activity depended on the ordering of task blocks and null blocks, i.e., block order ANBN, ABN, AB, or order AN followed by BN.

Recommendations in the literature for optimal block length in an alternating boxcar design range from 14 to 20 seconds (Chein & Schneider, 2003; Aguirre & D'Esposito, 1999; Wüstenberg, Giesel & Strasburger, 2005; Skudlarski, Constable & Gore, 1999; Smith, Jenkinson, Beckmann, Miller & Woolrich, 2007). Further, to produce a strong and homogeneous signal, it is optimal for detection to use a short time interval between the presentation of stimuli inside blocks, i.e., short stimulus asynchrony (SOA) (Chein & Schneider, 2003; Josephs & Henson, 1999). However, the duration of this interval depends on stimulus duration and the type of stimulus, e.g., a block with a mental rotation task may need a longer time between presentation of trials than a block with trials of a lexical decision task (Chein & Schneider, 2003).

The approach by Nakai et al. (2003) of fixing the number of task blocks and varying the number of null blocks resulted in different total experimental time periods for each design. In contrast, in our study a fixed time period for the experiment was assumed to determine which design is optimal within a fixed time period and resultant fixed budget. Additional to the block order, the optimization was expanded to other design factors, i.e., stimulus onset asynchrony (SOA) and block length which are displayed in Figure 1b. The SOA gives the time between presentation of two stimuli. To our knowledge, there is no study which has considered the optimization of blocked designs considering the influence from several varying design factors simultaneously, i.e., SOA, block length, and block order.

This optimization depends on the statistical model for the analysis of fMRI data and the optimality criterion. The general linear model is employed to model fMRI data at one three-dimensional imaging unit (Friston, Holmes, Poline, Grasby, Williams, Frackowiak & Turner,

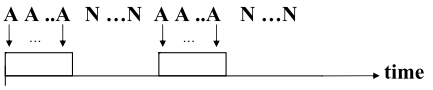

(a) Illustration of alternating boxcar design, A denotes task (stimulus) block and N a null (rest) block.

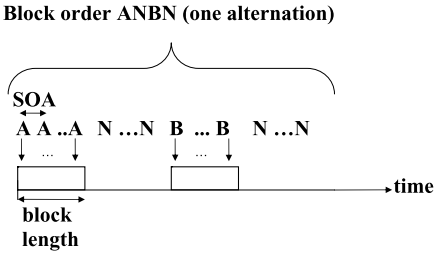

(b) Illustration of design factors, A and B denote task (stimulus) blocks whereas N denotes null (rest) block.

FIGURE 1.
Blocked designs.

1995). Several approaches to model the error have been undertaken, such as an uncorrelated error structure, which is the most simple case. However, it is known that fMRI data and the noise in fMRI data are temporally correlated and can thus be better fitted by a linear model with correlated error, notably autoregressive error of order 1 (AR1) (Bullmore, Brammer, Williams, Rabe-Hesketh, Janot, David, Mellers, Howard & Sham, 1996; Worsley, 2005; Chatfield, 2003) and AR1 plus measurement error (AR1+ME) (Purdon & Weisskoff, 1998). Ignoring autocorrelation will bias hypothesis-testing and confidence interval estimation as the error covariance matrix and the degrees of freedom of test statistics are incorrectly estimated (Worsley & Friston, 1995; Bullmore et al., 1996; Purdon & Weisskoff, 1998). According to Gautama and Van Hulle (2005) AR1 is the most frequently applied.

In the literature several optimality criteria were proposed which are all functions of the covariance matrix of the parameter estimators in the linear model. In this paper, the determinant or D-optimality criterion, the trace or A-optimality criterion, and the contrast or c-optimality criterion (Atkinson & Donev, 1996, Chapters 4, 10; Silvey, 1980) were used, and these will be explained in Section 3.1. As far as we know, the D-optimality criterion, has not been considered before for optimization of fMRI experiments. Methods from signal processing like power spectrum analysis have been applied to determine the optimal block length (Aguirre & D'Esposito, 1999), whereas the A-optimality criterion has mostly been applied for optimization of event-related designs (Dale, 1999; Friston et al., 1999; Liu et al., 2001; Liu & Frank, 2004; Wager & Nichols, 2003; Kao et al., 2009). Friston et al. (1999) have also used the c-optimality criterion to optimize detection power for contrasts between stimulus effects.

However, A-, D-, and c-optimal designs depend here on the model parameters, e.g., the autocorrelation in an AR1 error structure, and are thus only locally optimal. This problem will be solved by using the maximin criterion based on a relative efficiency measure. The maximin approach has been applied in optimal design theory to construct designs which are robust against misspecification of parameters in various models, e.g., the linear mixed model (Berger & Tan, 2004; Ouwens, Tan & Berger, 2002) or exponential regression models (Dette, Martinez Lopez, Ortiz Rodriguez & Pepelyshev, 2006). The effect of autocorrelation on optimal design has been studied before in the fMRI literature by assuming fixed parameter values in the error structure or by using real fMRI noise (Aguirre & D'Esposito, 1999; Smith et al., 2007; Wager & Nichols,

2003; Zarahn & Friston, 2002; Buračas & Boynton, 2002; Burock & Dale, 2000). As a result, the found optimal designs may not be robust against misspecification of these parameters.

To summarize, the objective of this paper is to determine the optimal blocked design for fMRI studies with respect to detection power. Three design factors, namely block length, ordering of blocks, and time between trials within one block, will be considered simultaneously to find the optimal combination of these factors. The time period of the experiment is assumed to be fixed. Furthermore, the maximin criterion is applied to solve the problem of local optimality due to a temporally correlated noise structure.

The outline of this paper is as follows. In Section 2.1 the general linear model is presented. For numerical calculations, a specific hemodynamic response function was chosen, which is introduced in Section 2.1. The different covariance matrices according to the different error structures are explained in Section 2.2. The results of our analysis of a blocked experiment are presented in Section 2.3, confirming the assumptions made in Section 2.1. The different optimality criteria, the maximin criterion, and the chosen values for the design factors SOA, block length, and block order are presented in Section 3. The results are described in Section 4 separately for the different error structures and optimality criteria. Finally, in Section 5 results are discussed, and conclusions are presented.

2. Model

2.1. General Linear Model

Considering an experiment with two stimulus types A and B, the fMRI signal Y at one voxel of one subject can be described by a general linear model (GLM). A voxelwise analysis is then performed, where one voxel corresponds to one three-dimensional imaging unit, for instance, 3 mm × 3 mm × 3 mm, in the subject's brain. The model is of the form

$$Y_i = X_{i1}\beta_0 + X_{i2}\beta_1 + X_{i3}\beta_2 + X_{i4}\beta_3 + \varepsilon_i, \tag{1}$$

where Y_i refers to the signal at time point i $(i = 1, \ldots, n)$, and n is the number of time points of the experiment. By the model in Equation (1), one fMRI run which is one continuously scanned time period can be described. The signal is normally sampled within the range of 5–10 min to avoid subject's fatigue and with a repetition time (TR) of several seconds, e.g., 2–4 s, to guarantee full brain coverage (Henson, 2004). The unknown parameters are the intercept β_0, effects β_1 and β_2 of stimuli A and B, and an effect β_3 for linear trend. The main interest is in the stimulus effects β_1 and β_2. In addition, a random error ε_i is present. The expected hemodynamic responses at time point i are reflected by X_{i2} and X_{i3}, the linear trend is modeled by regressor $X_{i4} = (i-1)\cdot \mathrm{TR} + 1\ \forall i$, and the fMRI baseline signal by $X_{i1} = 1\ \forall i$.

To calculate the hemodynamic response, a specific hemodynamic response function has to be assumed. In this paper, the sum of two gamma functions was applied (Friston et al., 1998):

$$\mathrm{h}(t) = \frac{b_1^{a_1+1}\cdot t^{a_1}\cdot \exp(-b_1 t)}{\Gamma(a_1+1)} - \frac{b_2{}^{a_2+1}\cdot t^{a_2}\cdot \exp(-b_2 t)}{c\cdot \Gamma(a_2+1)} \tag{2}$$

with parameters a_1, b_1, c, a_2, and b_2, where a_1/b_1 gives the time to the maximum for the positive gamma function (time to peak), and a_2/b_2 gives the time to the minimum for the negative gamma function (time to undershoot). Parameter c influences the ratio of the amplitudes of the positive and negative gamma function (peak-to-undershoot amplitude ratio). The first gamma function, known as the positive gamma function, models the peak of the hemodynamic response, while the second gamma function, the negative gamma function, models an undershoot. The HRF was

parameterized by $a_1 = 5, b_1 = 1$, $c = 6$, $a_2 = 15$, and $b_2 = 1$ that are appropriate for a brief stimulus (Henson, 2004), e.g., 1 s. The resulting HRF can be seen in Figure 2a. Additionally, it is common to assume that the hemodynamic response acts as the output of a linear time-invariant system (LTI) (Boynton, Engel, Glover & Heeger, 1996; Cohen, 1997; Dale & Buckner, 1997; Henson, 2004). Linearity means that the property of superposition is fulfilled so that the hemodynamic responses to successive stimuli are summed up to the final hemodynamic response

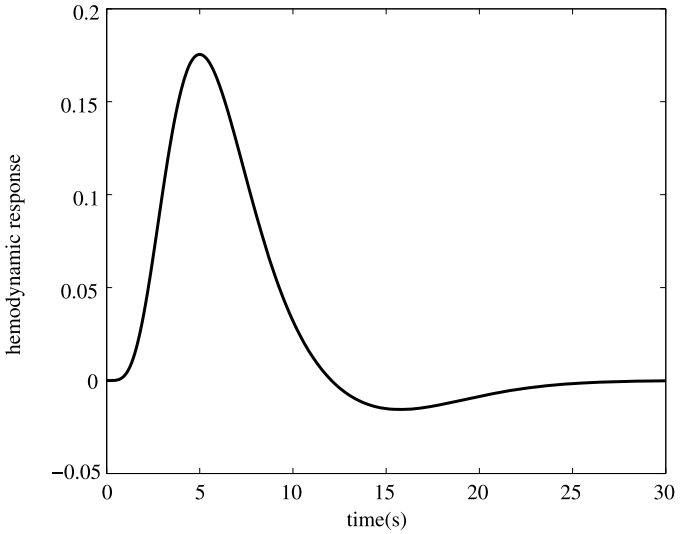

(a) Hemodynamic response function as sum of two gamma functions after presentation of stimulus A at 0 s.

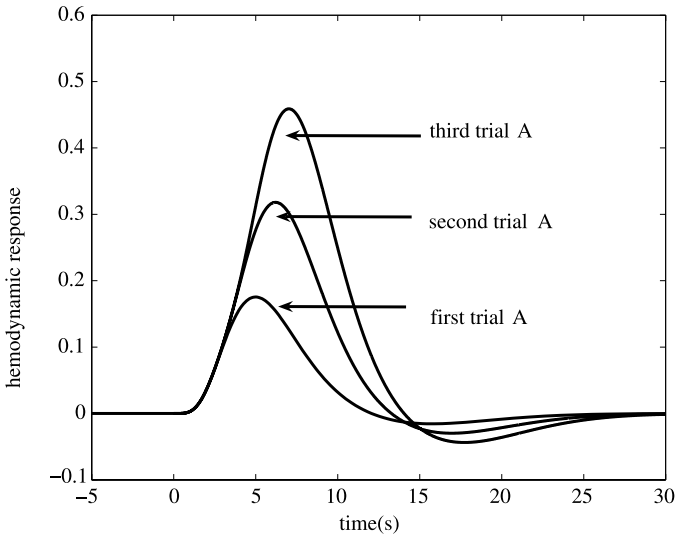

(b) Linearity of hemodynamic response after presentation of stimulus A at 0 s, 2 s and 3 s.

FIGURE 2.
Hemodynamic response.

as illustrated in Figure 2b. Invariance implies that the form of the hemodynamic response is independent of time (Henson, 2004).

Assuming linearity, invariance, and a specific HRF, the expected hemodynamic response X_{ij} at time point i to stimulus A, resp. B, can then be described mathematically by convolution to model the enduring hemodynamic response function after stimulus presentation and the superposition of hemodynamic responses to successive stimuli. The following equation gives the convolution $\mathbf{s} \otimes \mathbf{h}$ of a stimulus vector $\mathbf{s}_{\mathrm{A}}$, resp. $\mathbf{s}_{\mathrm{B}}$, with the HRF vector $\mathbf{h}$ at time point i:

$$X_{i2} = (s_{\mathrm{A}} \otimes \mathbf{h})(i) = \sum_{l=1}^{k+1} s_{\mathrm{A}}(i - l + 1)\mathbf{h}(l), \tag{3}$$

$$X_{i3} = (s_{\mathrm{B}} \otimes \mathbf{h})(i) = \sum_{l=1}^{k+1} s_{\mathrm{B}}(i - l + 1)\mathbf{h}(l). \tag{4}$$

The vectors $\mathbf{s}_{\mathrm{A}}$ and $\mathbf{s}_{\mathrm{B}} \in \mathbb{R}^n$ have entries 0 and 1, where 0 indicates no stimulus presentation of A, resp. B, at time point i, and 1 indicates a stimulus presentation of A, resp. B, at time point $i, i = 1, \ldots, n$. The HRF vector $\mathbf{h}$ represents the hemodynamic response function sampled at $0, 1\mathrm{TR}, 2\mathrm{TR}, \ldots, k\mathrm{TR}$, where $k + 1$ is the assumed number of time points for the hemodynamic response function.

In matrix notation, the general linear model in Equation (1) can be written as

$$Y = \mathrm{X}\beta + \varepsilon. \tag{5}$$

The vector $Y = (Y_1, \ldots, Y_n)^T$ is the fMRI signal, while β is the vector of the parameters $\beta_0, \beta_1, \beta_2$, and β_3. The design matrix X is an $n \times 4$ matrix and contains the entries X_{ij} in the jth column. The errors ε are assumed to be normally distributed with covariance matrix $\mathrm{cov}(\varepsilon)$.

The generalized least squares (GLS) estimator of β is given by

$$\hat{\beta} = \left[\mathrm{X}^T \mathrm{cov}(Y)^{-1} \mathrm{X}\right]^{-1} \mathrm{X}^T \mathrm{cov}(Y)^{-1} Y. \tag{6}$$

The GLS estimator is the best linear unbiased estimator. Assuming the errors to be normally distributed, it is also the maximum likelihood estimator. The 4×4 covariance matrix of $\hat{\beta}$ is equal to

$$\mathrm{cov}(\hat{\beta}) = \left[\mathrm{X}^T \mathrm{cov}(Y)^{-1} \mathrm{X}\right]^{-1}. \tag{7}$$

2.2. *Covariance Structure*

Three different covariance structures for the errors in Equation (1) were considered, always assuming the error to be normally distributed. Firstly, the error in the voxelwise GLM was assumed to follow an AR1 structure (Chatfield, 2003):

$$\varepsilon_{1,i} = \rho\, \varepsilon_{1,i-1} + \delta_{1,i} \quad \forall i \in \{1, \ldots, n\}, \tag{8}$$

where $\rho \in (-1, 1)$ and $\delta_{1,i} \sim N(0, \sigma_1^2)\ \forall i$ are independent identically distributed, i.e., uncorrelated noise. The AR1 model involves stationarity, which means that $E(\varepsilon_{1,i}) = 0$ and $\mathrm{var}(\varepsilon_{1,i}) = \sigma^2\ \forall i \in \{1, \ldots, n\}$. Another property of AR1 is that the covariance of the errors decreases with their separation in time: $\mathrm{cov}(\varepsilon_{1,i}, \varepsilon_{1,j}) = \rho^{|i-j|} \cdot \sigma^2$, where $|\rho| < 1$ and $i, j = 1, \ldots, n$. The symbol ρ denotes the autocorrelation parameter.

Secondly, AR1+ME was considered for the error structure, and thirdly, uncorrelated error (UE). The AR1+ME model is described by the equation

$$\varepsilon_{2,i} = \varepsilon_{1,i} + \delta_{2,i} \quad \forall i \in \{1, \ldots, n\}, \tag{9}$$

where $\varepsilon_{1,i}$ is defined as in Equation (8), and $\delta_{2,i}$ $\forall i$ are normally distributed with expectation 0 and variance σ_2^2 and are independent identically distributed. AR1+ME is more general than AR1, whereas UE is a special case of AR1 and AR1+ME. In the fMRI literature, AR1+ME is often referred to as AR1 plus white noise (Purdon & Weisskoff, 1998); and the AR1 term in Equation (8) is supposed to model the correlated structure of fMRI noise, whereas the measurement error δ_2 models scanner noise.

The covariance matrix $\text{cov}(\varepsilon_2)$ for AR1+ME consists of the covariance matrix $\sigma^2\text{V}$ for the AR1 term plus a covariance matrix for the measurement error δ_2. Thus, the covariance matrix of ε_2 is given by $\text{cov}(\varepsilon_2) = \sigma^2\text{V} + \sigma_2^2\text{I}_n$, where $V_{ij} = \rho^{|i-j|}$ for $i, j \in \{1, \ldots, n\}$, and I_n is the identity matrix of dimension n. The correlation between two errors is then given by $\text{corr}\,(\varepsilon_{2,i}, \varepsilon_{2,j}) = \frac{\sigma^2\rho^{|i-j|}}{\sigma^2+\sigma_2^2}$.

2.3. *Checking of Assumptions*

Assumptions about the specific form of the HRF and the linearity of the HRF were made in Section 2.1. It is known that there are problems of linearity for rapidly following trials. Dale and Buckner (1997) showed that for an SOA equal to 2 s, hemodynamic responses of stimuli add in a roughly linear way, but subtle deviations from linearity were obtained. One result of nonlinearity is a decrease in the amplitude, i.e., the hemodynamic response received by assumption of linearity is higher than the real hemodynamic response. This effect is called saturation (Henson, 2004). Furthermore, the shape of the hemodynamic response is slightly changed (Dale & Buckner, 1997).

While nonlinearity is a complex issue of which the causes and behavior are not completely understood, the reduction of amplitude for following trials in a sequence of events has been consistent in studies (Pollmann, Wiggins, Norris, von Cramon & Schubert, 1998; Huettel & McCarthy, 2000; Miezin, Maccotta, Ollinger, Peterson & Buckner, 2000; Wager, Vazquez, Hernandez & Noll, 2005). We decided to consider the effect of amplitude reduction by scaling the amplitude of the HRF. This is a simple approach to nonlinearity, which has already been applied by Wager and Nichols (2003) and Heckman, Bouvier, Carr, Harley, Cardinal, and Engel (2007).

Data from a blocked experiment were used to check our assumptions about the hemodynamic response and the AR1 model. The fMRI data were acquired with a gradient-echo EPI sequence (TE = 60 ms, FA = 90°, TR = 2000 ms, FOV = 200 × 200 mm, voxel size = 1.6 mm × 1.6 mm × 3 mm, 250 scans) and are an extended version of the experiment described in Formisano, Esposito, Di Salle, and Goebel (2004). Their experiment had two experimental conditions (left and right hemifield visual stimulation) alternated with fixation blocks, while our data were derived from an experiment with three experimental conditions (left, right, and both hemifield visual stimulation) alternated with fixation blocks.

Colored images of natural objects were presented to one healthy subject for 1 s within a stimulation block and directly replaced by the next image without an interstimulus interval (Formisano et al., 2004). Further details on experimental procedures and materials can be found in Formisano et al. (2004) and Goebel, Muckli, Zanella, Singer, and Stoerig (2001). The task blocks were of length 36 s, whereas the fixations blocks were of length 14 s or 18 s. Preprocessing was performed using Brain Voyager QX (Brain Innovation, Maastricht, The Netherlands, www.brainvoyager.com) and included 3D motion correction, slice-time correction, and a high-pass filter (including linear trend removal) in the time domain. Finally, the data were transformed to the Talairach space. The averaged time course from a region of interest (ROI) consisting of a volume of 773 mm^3 was analyzed.

The assumption about the error structure was checked on the residuals of this time series after fitting a general linear model with uncorrelated errors. The residuals could be better described by an AR1 structure than by uncorrelated error or moving average (MA). Fur-

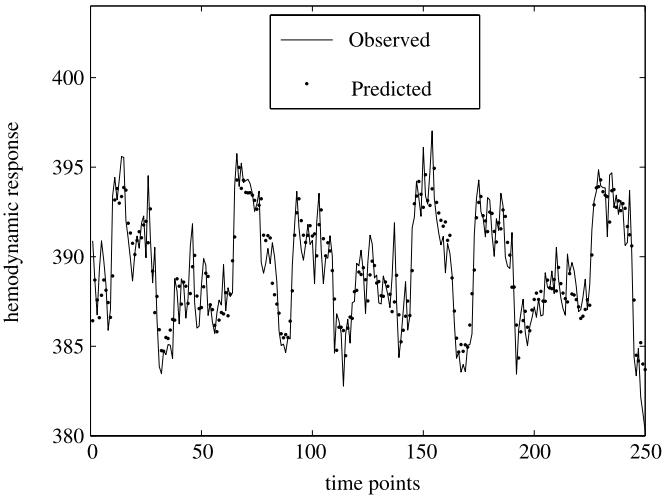

FIGURE 3.
Observed time course from region of interest of blocked experiment described in Section 2.3 and predicted time course from the general linear model based on double gamma function and AR1 error structure.

thermore, the assumption of the specific form of the HRF was controlled by assuming different HRF models from the literature (Cohen, 1997; Boynton et al., 1996) instead of the double gamma function. We fitted the data from the blocked experiment by a general linear model based on the double gamma function in Equation (2) with $a_1 = 5$, $b_1 = 1$, $c = 6$, $a_2 = 15$, and $b_2 = 1$ and by general linear models based on single gamma functions (Boynton et al., 1996; Cohen, 1997). The single gamma function of Boynton et al. (1996) was parameterized by $n = 3$, $\delta = 2.5$, and $\tau = 1.25$; and the single gamma function of Cohen was parameterized by $k = 1$. The double gamma function fitted the data slightly better with an R-square equal to 0.70, whereas the single gamma functions as applied by Boynton et al. (1996) or Cohen (1997) resulted in an R-square of 0.65 or 0.67.

Furthermore, different parameter values for the double gamma function were applied to check for effects of nonlinearity on the HRF shape in our data. However, the R-square values showed that the canonical parameter set described the HRF best. Figure 3 shows the observed time course in the region of interest and the predicted time course from our general linear model based on a double gamma function and AR1 error structure. It can be seen that a good fit to the observed time course is given by our predicted time course. The double gamma HRF with AR1 noise was therefore used in the sequel for design optimization.

3. Methods

Computations were performed with MATLAB (The MathWorks Inc., Natick, MA), and the default double gamma function from the MATLAB toolbox BVQXtools_v07b (Brain Innovation, Maastricht, The Netherlands) was applied. The MATLAB code is available upon request from the first author. Measurements of Y_i were supposed to be taken with a sampling rate, repetition time (TR), of 2 seconds. Covariance matrices $\text{cov}(\hat{\beta})$ were obtained by numerical computations using Equation (7) based on the values for the error parameters described in Section 3.3 and the values for the design factors given in Section 3.4. The covariance matrices are independent of a specific value of the $\beta's$ as Equation (7) shows.

3.1. Optimality Criteria

Considering general linear models, each design ξ in the design space Ξ results in a specific design matrix X_ξ. In our case, the design space Ξ was finite and consisted of blocked designs characterized by the factors SOA, block length, and block order. We will denote by $\hat{\beta}_\xi$ the estimator of β in Equation (6) which was obtained by the design matrix X_ξ of design ξ.

The D-optimal design minimizes the determinant of the covariance matrix $\text{cov}(\hat{\beta})$ (Atkinson & Donev, 1996, Chapter 10),

$$\text{Det}\big[\text{cov}(\hat{\beta}_\xi)\big] = \text{Det}\big\{\big[X_\xi^T \text{cov}(\varepsilon)^{-1} X_\xi\big]^{-1}\big\} \tag{10}$$

over all designs ξ in Ξ. One important property of the D-optimal design is that it results in minimizing the volume of the confidence ellipsoid of the parameters. Furthermore, the optimal design remains unchanged for different scaling of the variables in the design matrix X. The D-optimality criterion is frequently applied in many research areas because of these two useful properties.

If one is only interested in the variances of estimators, the A-optimality criterion may be used, which focuses on the trace of the covariance matrix $\text{cov}(\hat{\beta})$ (Atkinson & Donev, 1996, Chapter 10). A design is called A-optimal if it minimizes

$$\text{Tr}\big[\text{cov}(\hat{\beta}_\xi)\big] = \text{Tr}\big\{\big[X_\xi^T \text{cov}(\varepsilon)^{-1} X_\xi\big]^{-1}\big\} \tag{11}$$

over all designs ξ in Ξ. So, the A-optimal design minimizes the average variance of the parameter estimators.

The baseline effect β_0 and effect of linear trend β_3 are in general of no interest in fMRI research. We therefore use a special case of the L-optimality criterion (Atkinson & Donev, 1996, Chapter 10), which we will call the A_S-optimality criterion, and the D_S-optimality criterion to concentrate on a subset S of parameters (Atkinson & Donev, 1996, Chapter 10) $\beta^S = (\beta_1, \beta_2)^T$, which represents the stimulus effects of interest. The A_S-optimal design minimizes the trace of $\text{cov}(\hat{\beta}_\xi^S)$, whereas the D_S-optimal design minimizes the determinant of $\text{cov}(\hat{\beta}_\xi^S)$ for all designs ξ in Ξ.

By subtraction of effect parameters for two stimuli it can be determined which brain region is involved in a certain process. The area of seeing faces (Fusiform Face Area, FFA) is, e.g., detected by comparing the hemodynamic response to faces with the response to simple objects. Optimizing then means minimizing the variance of a parameter contrast and leads to a c-optimal design. The c-optimal design minimizes

$$\text{var}\big(c^T \hat{\beta}_\xi\big) = c^T \text{cov}(\hat{\beta}_\xi) c \tag{12}$$

for a given contrast vector $c^T \in \mathbb{R}^4$ with $\sum_{i=1}^4 c_i = 0$ over all designs ξ in the design space Ξ. Here, the difference $\beta_1 - \beta_2$ given by the contrast vector $c^T = (0, 1, -1, 0)$ is of interest. To summarize, five different optimal design criteria are applied: the D-, D_S-, A-, A_S-, and c-optimality criteria.

The relative efficiency (RE) can be used to compare a design ξ with the optimal design ξ^*. If we denote our optimality criterion by ψ, the relative efficiency of ξ versus ξ^* is defined as

$$\text{RE}(\xi | \xi^*) = \frac{\psi(\text{cov}(\hat{\beta}_{\xi^*}))}{\psi(\text{cov}(\hat{\beta}_\xi))}. \tag{13}$$

For the D- and D_S-optimality criteria, the pth root has to be taken, where p equals the number of parameters, i.e., $p = 4$ for β and $p = 2$ for β^S. By this, the relative efficiency has the same

interpretation for all optimality criteria, namely, that the inverse of the RE gives the number of times the design ξ has to be replicated to be as efficient as the optimal design. The relative efficiency of an arbitrary design versus the optimal design lies between 0 and 1, with a relative efficiency close to 1 being most desirable.

3.2. Maximin Approach

The covariance matrix $\text{cov}(\hat{\beta})$ depends on the parameters of the error structure, so the optimal design depends on ρ in the case of AR1 or on ρ and σ^2/σ_2^2 in the case of AR1+ME. This is called local optimality. There are several approaches to handle local optimality, e.g., the sequential approach (Silvey, 1980), the Bayesian design approach (Chaloner & Verdinelli, 1995; Atkinson & Donev, 1996, Chapter 19), and the maximin approach (Ouwens et al., 2002; Silvey, 1980, p. 59). Due to the high costs related to fMRI experiments, the sequential approach which needs several performances of experiments is not advantageous (Flaherty, Jordan & Arkin, 2006). The Bayesian approach requires assumptions about the prior distribution of the unknown parameters. For fMRI experiments, such a prior distribution is, however, not generally known for the parameters in the error structure. One disadvantage of the Bayesian approach is furthermore that the chosen optimal design may be efficient for the most likely parameter values but inefficient for a certain parameter value (Pronzato & Walter, 1988). Then the optimal design is not robust against misspecification of the parameter values.

The maximin approach maximizes the smallest relative efficiency and leads thereby to designs which are robust against misspecification of parameters if the maximum relative efficiency is high. We are searching for the maximin design (MMD) which fulfills the following condition in case of AR1 and for ρ in the parameter space $P_1 \subseteq [0, 1)$:

$$\text{MMD} = \arg \max_{\text{SOA,BL,BO}} \min_{\rho \in P_1} \text{RE}(\xi | \xi^*). \tag{14}$$

Firstly, given a certain optimality criterion and ρ, the optimal design ξ^* is determined. Secondly, for each design ξ with certain SOA, block length BL, and block order BO, the minimum relative efficiency (RE) is determined over the possible autocorrelation parameter values ρ in P_1. Thirdly, out of these minimum RE values the design with the largest value is chosen to be the maximin design for the optimality criterion. For AR1+ME and $\rho \times (\sigma^2/\sigma_2^2)$ in $P_1 \times P_2 \subseteq [0, 1) \times [0, +\infty)$, the condition is

$$\text{MMD} = \arg \max_{\text{SOA,BL,BO}} \min_{\rho \times \frac{\sigma^2}{\sigma_2^2} \in P_1 \times P_2} \text{RE}(\xi | \xi^*). \tag{15}$$

The maximum value in Equations (14) and (15) is called the maximin value (MMV).

3.3. Search for Locally Optimal Design

For AR1, the autocorrelation parameter ρ was varied by steps of 0.001 to detect optimal designs for a given ρ. We assumed ρ to lie in the interval [0, 0.5], as this range includes common values of correlation for two successive measurements Y_i and Y_{i+1}, respectively ε_i and ε_{i+1}, in fMRI data with TR = 2 s. For the AR1 model, ρ is the correlation of two successive data points, whereas for AR1+ME, the correlation is $\rho\sigma^2/(\sigma^2 + \sigma_2^2)$.

For AR1+ME, the ratio σ^2/σ_2^2 was considered to be 0.25, 0.5, 1, 2, and 4. In order to have a correlation of 0 to 0.5 between two adjacent measurements just as for AR1, we chose the autocorrelation parameter ρ to be in the interval [0, 0.7]. This results in a correlation of maximally 0.56 for all ratios of the variances. Lower values of the ratio will lead to an approximation of AR1+ME to the uncorrelated error structure, whereas higher values of the ratio will resemble the AR1 structure. The autocorrelation parameter was varied by steps of 0.01 to find an optimal design for a given ρ and given ratio σ^2/σ_2^2.

3.4. Design Factors

We chose to fix the stimulus duration at 1 s, thus not letting it play a role in our optimization. It is reasonable to choose an SOA close to the stimulus duration because this will result in a strong fMRI signal and no time between trials is wasted. Therefore, SOAs of 1, 2, and 3 seconds were applied.

Block length was the time from the first to the last trial in this block plus SOA. As block lengths usually lie between 10 s to 1 min (Chein & Schneider, 2003; Donaldson & Buckner, 2001), we covered this range by using 10, 15, 20, 30, and 60 s of block lengths. To test for the effect of the null blocks, we chose the following block orders: AB, ABN, and ANBN. The order of blocks is fixed for one design but repeated several times within the given time interval. For example, block order AB describes an experiment with repetition of AB (ABABABAB...) until the experiment is finished. In many studies it is necessary to use an active control condition instead of a resting condition. The null condition refers here to simple control conditions with no systematic or task-related activation, e.g., a fixation task or passive visual task, while more complex control conditions are considered as another task/stimulus type.

As time interval for the full modeled experiment, 720 s were needed because within this period, the block orders ANBN, AB, and ABN can be applied with several alternations and blocks of maximally 60 s. To cover the hemodynamic response to the last trial, the time period was finally expanded to 750 s for all designs resulting in 375 time points because TR was 2 s.

4. Results

4.1. Autoregressive Error of Order 1

The maximin design for all optimality criteria had block length equal to 15 s and an SOA of 1 s. For the D-, D_S-, and A_S-optimality criteria, the maximin design had block order ABN, for the A-optimality criterion, the maximin block order was ANBN, and for the c-optimality criterion, the block order was AB. The locally optimal designs had block lengths of 10 s, 15 s, or 20 s for some subintervals of $[0, 0.5]$ for ρ. Block length had a small effect on the minimum relative efficiency in comparison with block order and SOA. The effect of SOA was stronger than might be expected. As a result, for all optimality criteria except the D-optimality criterion, a design with SOA $= 2$ s resulted in only 25%–33% of the minimum relative efficiency of a design with SOA $= 1$ s, if block length and block order were kept constant. SOA $= 3$ s resulted in 11%–16% of the minimum relative efficiency of SOA $= 1$ s for all optimality criteria except the D-optimality criterion. For the D-optimality criterion, these values were 50% comparing an SOA of 2 s with an SOA of 1 s and 34% comparing 3 s with 1 s. The separate results from each optimality criterion are further described below and can be seen in Figure 4, which shows the minimum relative efficiencies for all designs and optimality criteria. Table 1 gives an overview of the maximin designs.

Since centering time X_{i4} in Equation (1) affects β_0 and thereby potentially may affect the A-optimal design, we also applied a centered linear trend, where $X_{i4} = (i - 1) \cdot \mathrm{TR} - 374\ \forall i$ instead of $X_{i4} = (i - 1) \cdot \mathrm{TR} + 1\ \forall i$ as for the following results. The variance of the intercept estimator $\mathrm{var}(\hat{\beta}_0)$ was smaller for the centered time trend, but this affected neither the locally optimal design nor the maximin design. For all optimality criteria, the locally optimal design and maximin design remained the same as for the uncentered time trend.

D- and D_S-Optimality Criteria The minimum relative efficiencies for the D-optimality criterion are presented in Figure 4a. The maximin value was equal to 0.97. Locally optimal were the designs with block length 10 s or 15 s, SOA $= 1$ s, and block order ABN, although there was

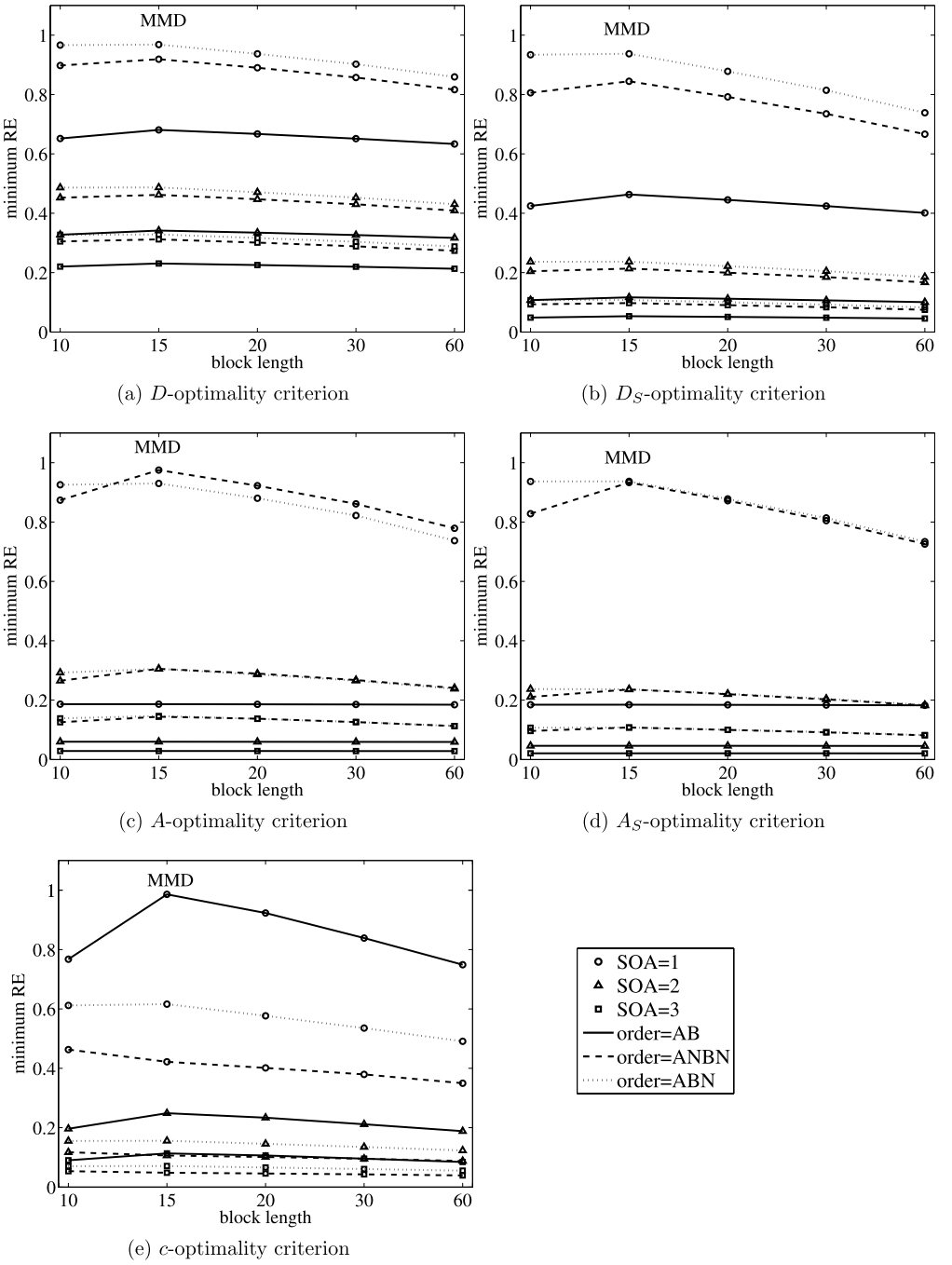

(a) D-optimality criterion

(b) D_S-optimality criterion

(c) A-optimality criterion

(d) A_S-optimality criterion

(e) c-optimality criterion

FIGURE 4.
Minimum relative efficiencies with AR1. MMD denotes the maximin design.

not much difference between ABN and ANBN. For all other block lengths than the optimal value 15 s, minimum relative efficiencies were slightly lower.

The results for the D_S-optimality criterion were similar to those for the D-optimality criterion, as can be seen in Figures 4a and 4b. For the D_S-optimality criterion, the maximin value was equal to 0.94. The only difference seemed to be in the height of the minimum relative efficiencies but not in the order of the various lines, i.e., designs. The same locally optimal designs and the same maximin design (SOA = 1 s, block length 15 s, and block order ABN) as for the D-optimality criterion were obtained.

A- and A_S-Optimality Criteria Figure 4c shows the minimum relative efficiencies for the A-optimality criterion. A-optimal were the designs with SOA = 1 s, BL = 10 s, 15 s, or 20 s and block order ANBN. The design with SOA = 1 s, block length 15 s, and block order ANBN was the maximin design. The A_S-optimality criterion gave similar results as the A-optimality criterion, except that the locally optimal designs and maximin design had block order ABN instead of ANBN, see Figure 4d. The maximin values were 0.97 for the A- and 0.94 for the A_S-optimality criterion. Differences in minimum relative efficiency between ABN and ANBN were mostly small for given SOA and block length.

For A- and A_S-optimality criteria and for D- and D_S-optimality criteria, it can be concluded from Figures 4a–4d that the designs with null blocks performed generally better than AB for any given SOA with little difference between ABN and ANBN. Furthermore, the effect of block length on minimum relative efficiencies was not large.

c-Optimality Criterion Figure 4e shows that the maximin design had order AB, SOA = 1 s, block length 15 s, and a maximin value of 0.99. Depending on ρ, the designs with SOA = 1 s, BL = 15 s or 20 s, and order AB were locally optimal. Block order AB was for any given block length and SOA more efficient than block order ABN, which in turn was more efficient than block order ANBN. The minimum relative efficiencies increased from block length 10 s to 15 s and decreased for higher block lengths than 15 s, except for order ANBN.

4.1.1. Costs of Choosing Nonoptimal Design Factors For the A-optimality criterion, the maximin design (BL = 15 s, SOA = 1 s, BO = ANBN) had a minimum relative efficiency of almost 1, whereas changing either block order or SOA to the least optimal value leads to minimum relative efficiencies smaller than 0.2. To exemplify the effect of choosing nonoptimal design factors in terms of costs, the results from the A-optimality criterion are therefore used as an extreme case. If the SOA of the maximin design is changed from 1 s to 3 s, the minimum relative efficiency becomes 0.14 in Figure 4c. This means that $1/0.14 \approx 7.14$ replications (7 runs) of this design (SOA = 3 s, BL = 15 s, block order = ANBN) are needed to be approximately as efficient as the maximin design. Assuming costs of \$600 per hour, \$875 instead of \$125 would have to be spent to obtain the same efficiency.

If the block order is changed to AB keeping SOA = 1 s and BL = 15 s, it can be calculated that about $1/0.19 \approx 5.26$ replications (five runs) are necessary to be nearly as efficient as the maximin design. With the same assumption of costs per hour as before, we obtain costs of \$625 instead of \$125. By changing the block length of the maximin design to 60 s, a minimum relative efficiency of 0.87 is obtained in Figure 4c and $1/0.78 \approx 1.28$ repetitions. Thus, the design with BL = 60 s is almost as efficient as the maximin design. In conclusion, SOA and block order had a strong effect on costs, whereas block length had a weak effect on costs for the A-optimality criterion.

4.1.2. Effect of Nonlinearity Based on the results by Binder, Rao, Hammeke, Frost, Bandettini, and Hyde (1994), the effect of nonlinearity on design efficiency was studied by assuming that the amplitude of the HRF was reduced to 81% of its canonical value in case of SOA = 1 s, while SOA = 2 s or 3 s were assumed to give rise to the canonical HRF. For the A-, D_S-, A_S-,

and c-optimality criteria, the minimum relative efficiency of SOA = 2 s was 38%–44% of the minimum relative efficiency of the same design with SOA = 1 s (block length and block order not changed), instead of 25%–33% for linearity. For the D-optimality criterion, a design with SOA = 2 s had 62% instead of 50% of the minimum relative efficiency of a design with SOA = 1 s. For the A-, D_S-, A_S-, and c-optimality criteria, SOA = 3 s resulted in 17%–21% of the minimum relative efficiency of SOA = 1 s instead of 11%–16% for linearity, while for the D-optimality criterion, this value was between 41% to 42% instead of 34%. In conclusion, an SOA equal to 1 s was still the most efficient, but the effect of the SOA on design efficiency was less strong if nonlinearity was taken into account.

4.2. Uncorrelated Errors and Autoregressive Errors Plus Measurement Error

For uncorrelated errors, the maximin approach is not needed because $\rho = 0$ and the optimal design can be determined by comparing the relative efficiencies directly. The results were similar to those of AR1 with two mentionable differences. Firstly, A-optimal was the design with SOA = 1 s, block order ANBN, and BL = 20 s instead of 15 s; and secondly, c-optimal was the design with SOA = 1 s, order AB, and BL = 20 s instead of 15 s, as can be seen in Table 1.

The same locally optimal designs as for AR1 were obtained for AR1+ME, except for the c-optimality criterion, which had locally optimal designs with block lengths 10 s, 15 s, 20 s, block order AB, and SOA = 1 s. Block length 10 s performed better than for AR1, as can be seen in Table 1; and the effect of block length was slightly stronger than for AR1 with a stronger decrease in minimum relative efficiencies for higher block length. Similarly to AR1, lower SOAs performed better than higher SOAs; and null blocks were preferred by the D-, D_S-, A-, and A_S-optimality criteria, whereas no null blocks were preferred by the c-optimality criterion.

Depending on both the ratio σ^2/σ_2^2 and the autocorrelation parameter ρ, the locally optimal design differed in block length. However, the locally optimal designs had always an SOA equal to 1 s and block length 10, 15, or 20 seconds for all optimality criteria. The locally optimal designs had block order ABN for the D-, D_S-, and A_S-optimality criteria, block order ANBN for the A-optimality criterion, and block order AB for the c-optimality criterion. The maximin designs can

TABLE 1.
Maximin designs for AR1 and AR1+ME and the optimal designs for uncorrelated errors (UE).

Optimality criterion	Error structure		
	AR1	UE	AR1+ME
D	SOA = 1 s, BL = 15 s, order = ABN	SOA = 1 s, BL = 15 s, order = ABN	SOA = 1 s, BL = 10 s, order = ABN
D_S	SOA = 1 s, BL = 15 s, order = ABN	SOA = 1 s, BL = 15 s, order = ABN	SOA = 1 s, BL = 10 s, order = ABN
A	SOA = 1 s, BL = 15 s, order = ANBN	SOA = 1 s, BL = 20 s, order = ANBN	SOA = 1 s, BL = 15 s, order = ANBN
A_S	SOA = 1 s, BL = 15 s, order = ABN	SOA = 1 s, BL = 15 s, order = ABN	SOA = 1 s, BL = 10 s, order = ABN
c	SOA = 1 s, BL = 15 s, order = AB	SOA = 1 s, BL = 20 s, order = AB	SOA = 1 s, BL = 15 s, order = AB

be seen in Table 1. For higher ratios of the variances σ^2/σ_2^2, AR1+ME behaved more similar to AR1 with regard to the locally optimal designs.

5. Discussion

The results of AR1 and AR1+ME did not differ much. This was expected as the AR1+ME error structure approaches AR1 for higher ratios σ^2/σ_2^2. Furthermore, for a smaller ratio of the variances, the AR1+ME structure is approximating uncorrelated errors, and UE gave also similar results as AR1. Therefore, the further discussion of results is restricted to the AR1 error structure.

The D-, D_S-, and A_S-optimality criteria gave very similar results with respect to the maximin design and the evaluation of block order ABN and ANBN. For all these optimality criteria, the maximin design was the design with SOA = 1 s, block length = 15 s, and block order ABN. Furthermore, block order ABN performed always slightly better than ANBN for a given SOA. The maximin designs for the A- and c- optimality criteria differed only in block order: ANBN for A- and AB for the c-optimality criterion.

The preference for block order AB of the c-criterion is in agreement with Smith et al. (2007), who showed that for estimating a contrast between two task blocks no rest period (no null block) is optimal. Similarly, Friston et al. (1999) found that for event-related designs, no null events should be used to estimate the differential contrast. In contrast, designs with null blocks were favored by the D-, D_S-, A-, and A_S-optimality criteria as null blocks are necessary for the estimation of β_0, β_1, and β_2.

Regarding SOA, we found that small SOAs resulted in higher values of the minimum relative efficiencies if the other design factors are constant. This was expected because more trials in one block cause an overlap of the hemodynamic responses leading to a higher total response which simplifies the detection of activated areas. However, the magnitude of the effect of SOA was larger than expected, e.g., for all optimality criteria except the D-optimality criteria, the minimum relative efficiency decreased from SOA = 1 s to SOA = 2 s by at least 67% (D-optimality criterion: exactly 50%) under linearity.

Optimal block lengths were 10 s, 15 s, or 20 s, but the effect of block length was small so that the minimum relative efficiency did not change much for different block lengths. The small effect of block length might be explained by the fact that only linear trends were considered, and no other trends or aspects of noise, e.g., physiological noise, were included in the model. On the other hand, the temporally correlated structure of fMRI noise is captured very well by AR1, and results do not differ much between uncorrelated and correlated errors.

A conclusion from the results of the A_S- and D_S-optimality criteria is that null blocks are recommendable to estimate the stimulus effects. To estimate the contrast between A and B, we would advise to apply the block order AB. If there is interest in estimating the stimulus effects and contrasts, order ABN will be a good choice as it outperformed ANBN in the results from the c-optimality criterion and performed comparably to ANBN for the other optimality criteria. Optimal stimulus onset asynchrony (SOA) should be as small as possible, and an optimal block length should be in the range of 10 s to 20 s. However, the effect of block length was not strong in comparison with the effect of SOA or block order. Thus, in planning an fMRI experiment, a researcher may first decide on an appropriate SOA, then on the block order depending on the effects or contrasts of interest, and finally on block length.

With respect to the choice of optimality criterion, the A- and A_S-optimality criteria were already applied in fMRI research (Dale, 1999; Liu et al., 2001; Wager & Nichols, 2003), but there is no reason to generally prefer A- over D-optimality concerning the optimization of fMRI experiments. An advantage of the A-optimality criterion is that the parameter estimators can be

linearly weighted in the trace function (Conlisk & Watts, 1979) if there is more interest in one parameter than in the other, but that was not the case in this study.

One often cited advantage of the D-optimality criterion is the independence of the D-optimal design with respect to the scaling of the regressors. Furthermore, the D-optimal design results in a minimized confidence ellipsoid for the unknown parameters. A disadvantage is that the D-optimal design may lead to minimization of the confidence ellipsoid in only one direction and strong elongation of the ellipse along one axis (Sim & Roy, 2005; Atkinson & Donev, 1996, p. 106). This can occur if the trials of the two stimuli A and B are not presented equally often or if var(ε) is assumed to be heterogeneous. The comparable results of the A_S- and D_S- optimality criteria for the maximin designs and locally optimal designs may be explained by the homogeneity of the error variance and the fact that the regressors for stimulus effects were time-shifted versions of each other. Modeling heterogeneity or unequal number of trials is, however, beyond the scope of this paper.

So, for this study, there is no obvious choice between the A- or D-optimality criteria. We do, however, recommend restricting to the optimization of the stimulus effects' estimation, in particular if more confounders are included in the model, e.g., quadratic trend effects. Thus, the following optimality criteria remain: the c-optimality criterion for estimation of contrasts and the A_S- or D_S-optimality criterion. Since the D_S-optimality criterion results in a minimized confidence ellipsoid of the estimators of interest, we prefer this optimality criterion for our modeled experiment.

Further research is needed to determine to which extent the results depend on the parameterization of the double gamma function. For example, the optimal block length might increase if the hemodynamic response function is more broad, and thus the power spectrum of the HRF is higher at low frequencies. Liu et al. (2001) showed this for uncorrelated errors, but more research also with correlated errors is needed. Furthermore, the optimal block order could differ if the length and the strength of the undershoot is changed, e.g., more null blocks might be necessary for a longer undershoot.

Another important aspect for further research is the extension of our model to mixed effects models and the optimization of designs for second level analysis, which is nowadays common in fMRI data analysis. Random effects are necessary to generalize inferences to the population from which subjects are drawn. With regard to optimization of designs for these models, the covariance matrix cov($\hat{\beta}$) in Equation (7) has to be adjusted by taking inter-subject and intra-subject variance into account.

Acknowledgement

The authors want to thank Fabrizio Esposito for help with the data analyses. The first author is supported by the Netherlands Organisation for Scientific Research (NWO/MAGW, grant number 400-05-063).

References

Aguirre, G.K., & D'Esposito, M. (1999). Experimental design for brain fMRI. In C.T.W. Moonen, & P.A. Bandettini (Eds.), *Functional MRI* (pp. 369–380). Berlin: Springer.

Atkinson, A.C., & Donev, A.N. (1996). *Optimum experimental designs*. Oxford: Clarendon.

Berger, M.P.F., & Tan, F.E.S. (2004). Robust designs for linear mixed effects model. *Applied Statistics*, *53*(4), 569–581.

Binder, J.R., Rao, S.M., Hammeke, T.A., Frost, J.A., Bandettini, P.A., & Hyde, J.S. (1994). Effects of stimulus rate on signal response during functional magnetic resonance imaging of auditory cortex. *Cognitive Brain Research*, *2*, 31–38.

Birn, R.M., Cox, R.W., & Bandettini, P.A. (2002). Detection versus estimation in event-related fMRI: choosing the optimal stimulus timing. *NeuroImage*, *15*, 252–264.

Boynton, G.M., Engel, S.A., Glover, G.H., & Heeger, D.J. (1996). Linear systems analysis of functional magnetic resonance imaging in human V1. *The Journal of Neuroscience*, *16*(13), 4207–4221.

Buckner, R.L., Bandettini, P.A., O'Craven, K.M., Savoy, R.L., Petersen, S.E., Raichle, M.E., & Rosen, B.R. (1996). Detection of cortical activation during averaged single trials of a cognitive task using functional magnetic resonance imaging. *Proceedings of the National Academy of Sciences of the United States of America*, *93*, 14878–14883.

Bullmore, E., Brammer, M., Williams, S.C.R., Rabe-Hesketh, S., Janot, N., David, A., Mellers, J., Howard, R., & Sham, P. (1996). Statistical methods of estimation and inference for functional MR image analysis. *Magnetic Resonance in Medicine*, *35*, 261–277.

Buračas, G.T., & Boynton, G.M. (2002). Efficient design of event-related fMRI experiments using M-sequences. *NeuroImage*, *16*, 801–813.

Burock, M.A., & Dale, A.M. (2000). Estimation and detection of event-related fMRI signals with temporally correlated noise: a statistically efficient and unbiased approach. *Human Brain Mapping*, *11*, 249–260.

Chaloner, K., & Verdinelli, I. (1995). Bayesian experimental design: a review. *Statistical Science*, *10*(3), 273–304.

Chatfield, C. (2003). *The Analysis of Time Series: An Introduction* (6th ed.). London/Boca Raton: Chapman and Hall/CRC Press.

Chein, J.M., & Schneider, W. (2003). Designing effective fMRI experiments. In J. Grafman, & I. Robertson (Eds.), *The handbook of neuropsychology*. Amsterdam: Elsevier.

Cohen, M.S. (1997). Parametric analysis of fMRI data using linear systems methods. *NeuroImage*, *6*, 93–103.

Conlisk, J., & Watts, H. (1979). A model for optimizing experimental designs for estimating response surfaces. *Journal of Econometrics*, *11*, 27–42.

Culham, J.C. (2006). Functional neuroimaging: Experimental design and analysis. In R. Cabeza, & A. Kingstone (Eds.), *Handbook of functional neuroimaging of cognition* (pp. 53–82). Cambridge: MIT Press.

Dale, A.M. (1999). Optimal experimental design for event-related fMRI. *Human Brain Mapping*, *8*, 109–114.

Dale, A.M., & Buckner, R.L. (1997). Selective averaging of rapidly presented individual trials using fMRI. *Human Brain Mapping*, *5*, 329–340.

Dette, H., Martinez Lopez, I., Ortiz Rodriguez, I.M., & Pepelyshev, A. (2006). Maximin efficient design of experiment for exponential regression models. *Journal of Statistical Planning and Inference*, *136*, 4397–4418.

Di Salle, F., Formisano, E., Linden, D.E.J., Goebel, R., Bonavita, S., Pepino, A., Smaltino, F., & Tedeschi, G. (1999). Exploring brain function with magnetic resonance imaging. *European Journal of Radiology*, *30*, 84–94.

Donaldson, D.I., & Buckner, R.L. (2001). Effective paradigm design. In P. Jezzard, P.M. Matthews, & S.M. Smith (Eds.), *Functional MRI: an introduction to methods* (pp. 177–196). Oxford: Oxford University Press.

Flaherty, P., Jordan, M.I., & Arkin, A.P. (2006). Robust design of biological experiments. In Y. Weiss, B. Schölkopf, & J. Platt (Eds.), *Advances in neural information processing systems* (Vol. 18, pp. 363–370). Cambridge: MIT Press.

Formisano, E., Esposito, F., Di Salle, F., & Goebel, R. (2004). Cortex-based independent component analysis of fMRI time series. *Magnetic Resonance Imaging*, *22*, 1493–1504.

Friston, K.J., Fletcher, P., Josephs, O., Holmes, A., Rugg, M.D., & Turner, R. (1998). Event-related fMRI: characterizing differential responses. *NeuroImage*, *7*, 30–40.

Friston, K.J., Holmes, A.P., Poline, J.-B., Grasby, P.J., Williams, S.C.R., Frackowiak, R.S.J., & Turner, R. (1995). Analysis of fMRI time-series revisited. *NeuroImage*, *2*, 45–53.

Friston, K.J., Jezzard, P., & Turner, R. (1994). Analysis of functional MRI time-series. *Human Brain Mapping*, *1*, 153–171.

Friston, K.J., Zarahn, E., Josephs, O., Henson, R.N.A., & Dale, A.M. (1999). Stochastic designs in event-related fMRI. *NeuroImage*, *10*, 607–619.

Gautama, T., & Van Hulle, M.M. (2005). Estimating the global order of the fMRI noise model. *NeuroImage*, *26*, 1211–1217.

Goebel, R., Muckli, L., Zanella, F.E., Singer, W., & Stoerig, P. (2001). Sustained extrastriate cortical activation without visual awareness revealed by fMRI studies of hemianopic patients. *Vision Research*, *41*, 1459–1474.

Hagberg, G.E., Zito, G., Patria, F., & Sanes, J.N. (2001). Improved detection of event-related functional MRI signals using probability functions. *NeuroImage*, *14*, 1193–1205.

Heckman, G.M., Bouvier, S.E., Carr, V.A., Harley, E.M., Cardinal, K.S., & Engel, S.A. (2007). Nonlinearities in rapid event-related fMRI explained by stimulus scaling. *NeuroImage*, *34*, 651–660.

Henson, R.N.A. (2004). Analysis of fMRI time series. In R.S.J. Frackowiak, K.J. Friston, C.D. Frith, R.J. Dolan, C.J. Price, S. Zeki, J. Ashburner, & W. Penny (Eds.), *Human brain function* (pp. 793–822). Amsterdam: Elsevier.

Honey, G.D., & Bullmore, E.T. (2002). Functional neuroimaging and schizophrenia. *Psychiatry*, *1*, 26–29.

Huettel, S.A., & McCarthy, G. (2000). Evidence for a refractory period in the hemodynamic response to visual stimuli as measured by MRI. *NeuroImage*, *11*, 547–553.

Josephs, O., & Henson, R.N.A. (1999). Event-related functional magnetic resonance imaging: modelling, inference and optimization. *Philosophical Transactions of the Royal Society B*, *354*, 1215–1228.

Kao, M.-H., Mandal, A., Lazar, N., & Stufken, J. (2009). Multi-objective optimal experimental designs for event-related fMRI studies. *NeuroImage*, *44*, 849–856.

Liu, T.T. (2004). Efficiency, power and entropy in event-related fMRI with multiple trial types, part II: design of experiments. *Neuroimage*, *21*, 401–413.

Liu, T.T., & Frank, L.R. (2004). Efficiency, power, and entropy in event-related fMRI with multiple trial types, part I: theory. *NeuroImage*, *21*, 387–400.

Liu, T.T., Frank, L.R., Wong, E.C., & Buxton, R.B. (2001). Detection power, estimation efficiency, and predictability in event-related fMRI. *NeuroImage*, *13*, 759–773.

Logothetis, N.K., & Wandell, B.A. (2004). Interpreting the BOLD signal. *Annual Review of Physiology*, *66*, 735–769.
Maus, B., van Breukelen, G.J.P., Goebel, R., & Berger, M.P.F. (2010). Robustness of optimal design of fMRI experiments with application of a genetic algorithm. *NeuroImage*, *49*, 2433–2443.
Miezin, F.M., Maccotta, L., Ollinger, J.M., Petersen, S.E., & Buckner, R.L. (2000). Characterizing the hemodynamic response: effects of presentation rate, sampling procedure, and the possibility of ordering brain activity based on relative timing. *NeuroImage*, *11*, 735–759.
Mohamed, F.B., Tracy, J.I., Faro, S.H., Emperado, J., Koenigsberg, R., Pinus, A., & Tsai, F.Y. (2000). Investigation of alternating and continuous experimental task designs during single finger opposition fMRI: a comparative study. *Journal of Computer Assisted Tomography*, *24*(6), 935–941.
Nakai, T., Matsumura, A., Nose, T., Kato, C., Glover, G.H., & Matsuo, K. (2003). The effect of task block arrangement on the detectability of activation in fMRI. *Magnetic Resonance Imaging*, *21*, 941–947.
Ouwens, M.J.N.M., Tan, F.E.S., & Berger, M.P.F. (2002). Maximin D-optimal designs for longitudinal mixed effects model. *Biometrics*, *58*, 735–741.
Owen, A.M., Epstein, R., & Johnsrude, I.S. (2003). fMRI: applications to cognitive neuroscience. In P. Jezzard, P.M. Matthews, & S.M. Smith (Eds.), *Functional MRI: an introduction to methods* (pp. 311–327). Oxford: Oxford University Press.
Pollmann, S., Wiggins, C.J., Norris, D.G., von Cramon, D.Y., & Schubert, T. (1998). Use of short intertrial intervals in single-trial experiments: a 3T fMRI-study. *Neuroimage*, *8*, 327–339.
Pronzato, L., & Walter, E. (1988). Robust experimental design via maximin optimization. *Mathematical Biosciences*, *89*, 161–176.
Purdon, P.L., & Weisskoff, R.M. (1998). Effect of temporal autocorrelation due to physiological noise and stimulus paradigm on voxel-level false-positive rates in fMRI. *Human Brain Mapping*, *6*, 239–249.
Rosen, B.R., Buckner, R.L., & Dale, A.M. (1998). Event-related functional MRI: past, present and future. *Proceedings of the National Academy of Sciences*, *95*, 773–780.
Silvey, S. (1980). *Optimal design*. London: Chapman & Hall.
Sim, R., & Roy, N. (2005). Global A-optimal robot exploration in SLAM. In *Proceedings of the IEEE/RSJ international conference of robotics and automation (ICRA 2005)* (pp. 661–666).
Skudlarski, P., Constable, R.T., & Gore, J.C. (1999). ROC analysis of statistical methods used in functional MRI: individual subjects. *NeuroImage*, *9*, 311–329.
Smith, S., Jenkinson, M., Beckmann, C., Miller, K., & Woolrich, M. (2007). Meaningful design and contrast estimability in FMRI. *NeuroImage*, *34*, 127–136.
Wager, T.D., & Nichols, T.E. (2003). Optimization of experimental design in fMRI: a general framework using a genetic algorithm. *NeuroImage*, *18*, 293–309.
Wager, T.D., Vazquez, A., Hernandez, L., & Noll, D.C. (2005). Accounting for nonlinear BOLD effects in fMRI: parameter estimates and a model for prediction in rapid event-related studies. *NeuroImage*, *25*, 206–218.
Worsley, K.J. (2005). Spatial smoothing of autocorrelations to control the degrees of freedom in fMRI analysis. *NeuroImage*, *26*, 635–641.
Worsley, K.J., & Friston, K.J. (1995). Analysis of fMRI time-series revisited-again. *NeuroImage*, *2*, 173–181.
Wüstenberg, T., Giesel, F.L., & Strasburger, H. (2005). Methodische Grundlagen der Optimierung funktioneller MR-Experimente. *Radiologe*, *45*, 99–112.
Zarahn, E., & Friston, K.J. (2002). Some limit results for efficiency in stochastic fMRI designs. *Biometrical Journal*, *44*, 496–509.

Manuscript Received: 2 SEP 2009
Final Version Received: 27 NOV 2009
Published Online Date: 23 MAR 2010